

Supplementary Information

Benchtop Fabrication of Three-Dimensional Reconfigurable Microfluidic Devices from Paper/Polymer Composite

Yu Long Han^{a,b}, Wenqi Wang^{a,b}, Jie Hu^{a,b}, Guoyou Huang^{a,b}, Shuqi Wang^c,
Won Gu Lee^d, Tian Jian Lu^{b*}, Feng Xu^{a,b*}

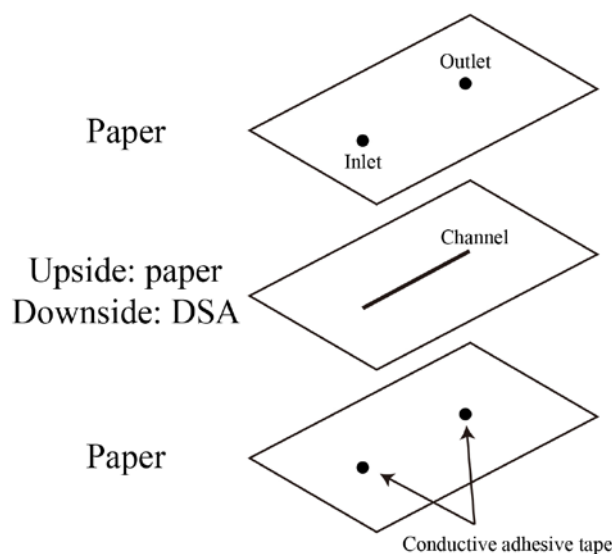


Fig. S1 Design of the straight channel for reconfigurable circuit.

1. Quantification of width changes caused by PDMS infiltration

We took photos of channel at the same place before and after PDMS infiltration (**Fig. 4C-D**). The width along the channel was quantified from the photos using Image pro plus 6.0 (IPP) at ten points (**Fig. S2A**). The average width of channel and standard deviation were presented in **Fig. S2B**. The paired sample *t* test was used to analyze the difference between these two samples, from which we did not observe significant difference.

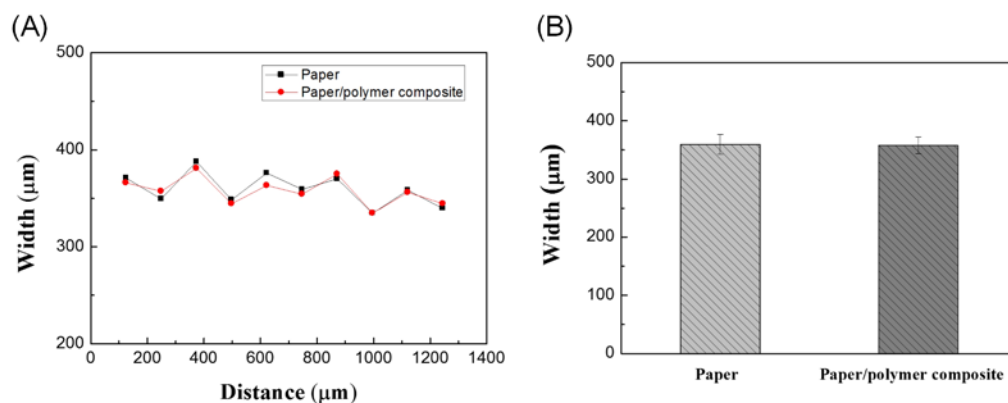


Fig. S2 Quantification of width changes caused by PDMS infiltration. (A) Width changes along the channel before and after PDMS infiltration. (B) Comparison of average width before and after PDMS infiltration.

2. Evaluation of paper ablation caused by laser etching

The ablation of paper using laser may also affect the channel width, especially for small sized channels. To evaluate this effect, we etched a straight line out from a layer of printing paper using different laser powers. The power of laser etcher was adjusted in the software from 10% to 100% (25 W laser source). At each power, three samples were used to fabricate channels. The speed of etching process was kept constant at 40% in the software for all the experiments.

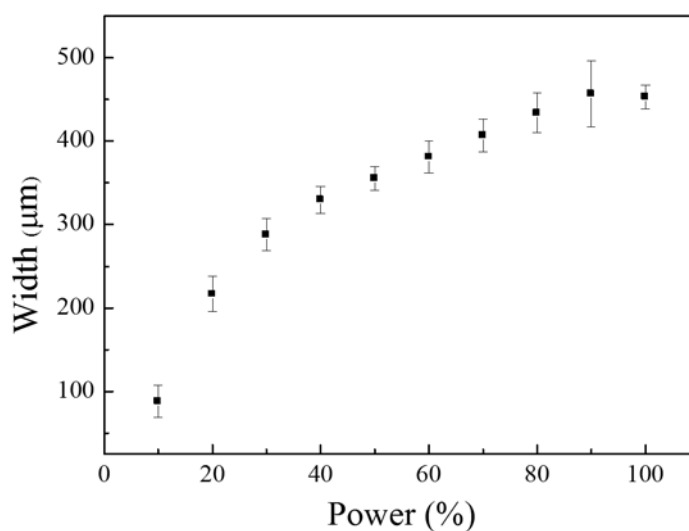


Fig. S3 Control the channel width by applied laser power.

3. Evaluation of thickness uniform along the whole structure

To investigate the effect of dripping and flowing of PDMS on the thickness uniformity along the whole structure, we measured the thickness variation in the cross section of the fabricated device, *i.e.*, a two-layered microchannel. The cross section was imaged using a digital microscope (VHX-600, Keyence Corporation, Japan) and the height was quantified using IPP. The results show that there was no significant variation in the thickness of the paper/polymer composite device (**Fig. S4**). The thickness of the device (*e.g.*, the channel height) was controlled by the thickness of the paper used (**Fig. 4E**). In the view of cross-section (**Fig. 4F**), we found that the height of channel was similar to the total height of paper and DSA, indicating that there was no obviously residual PDMS in the channel. For example, for a 2-layer channel, the channel height was composed of two 2 layers of paper (90 μm for one layer paper) and 2 layers of DSA (40 μm for one layer DSA). And the height of microchannel after PDMS infiltration was the same as the height of paper and DSA (249 \pm 9 μm v.s. 260 μm). Besides, the height of channel was uniform according to **Fig. S4**.

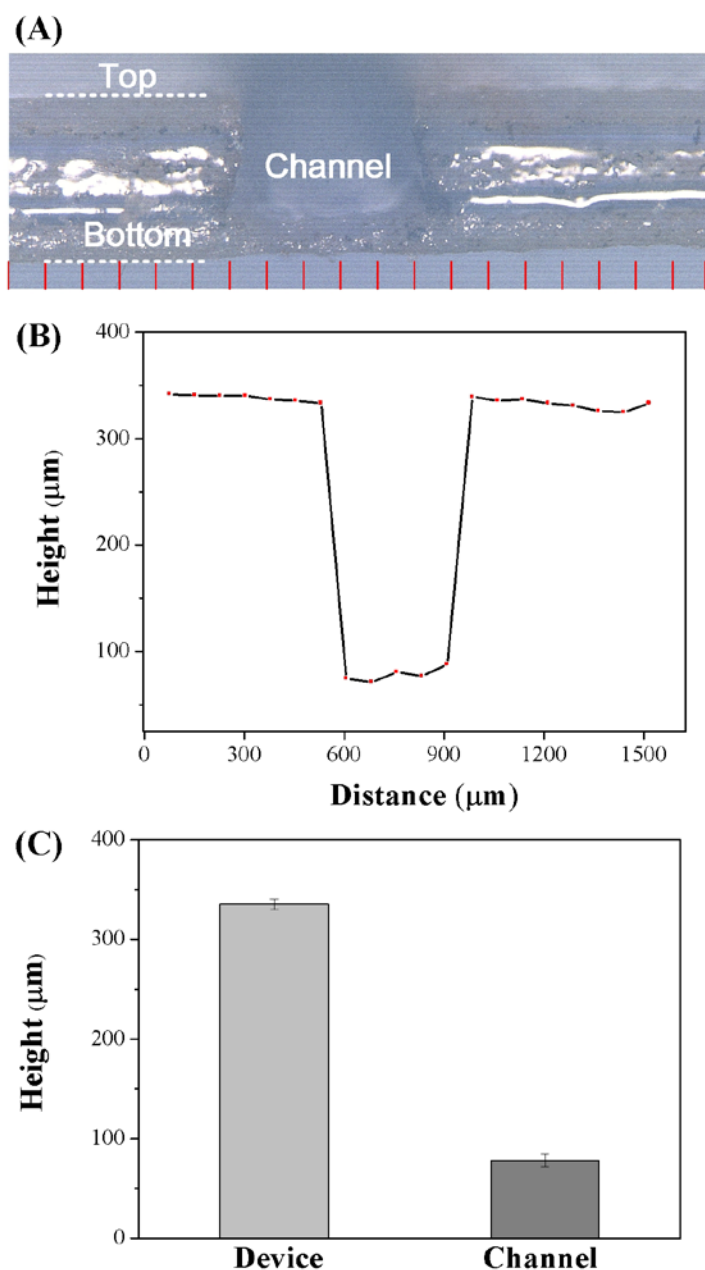


Fig. S4 Photograph of the cross-section of channel and analysis of the height of microfluidic device after PDMS infiltration. (A) Optical image of a two-layered channel. (B) Plot diagram for the height versus the distance measured along the whole cross-section of device. (C) Average height of the device and channel.

4. Surface changes of DSA before and after PDMS infiltration

To check how DSA reacts with PDMS, we compared the surface of DSA before and after PDMS infiltration (**Fig. S5**). No significant changes were observed from SEM images. The results indicate that the DSA has different reaction behaviors with PDMS from that with paper. To the best of our knowledge, the DSA is water and gas impermeable, thus we would not expect that PDMS can infiltrate into DSA.

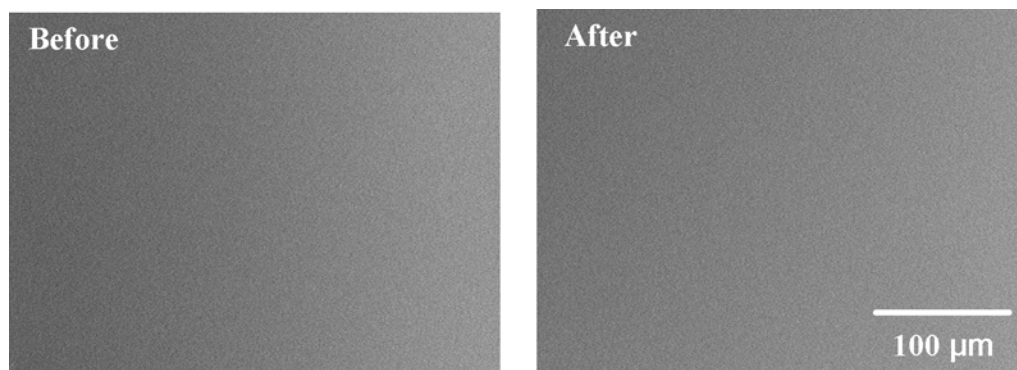


Fig. S5 SEM images of DSA before and after PDMS infiltration.

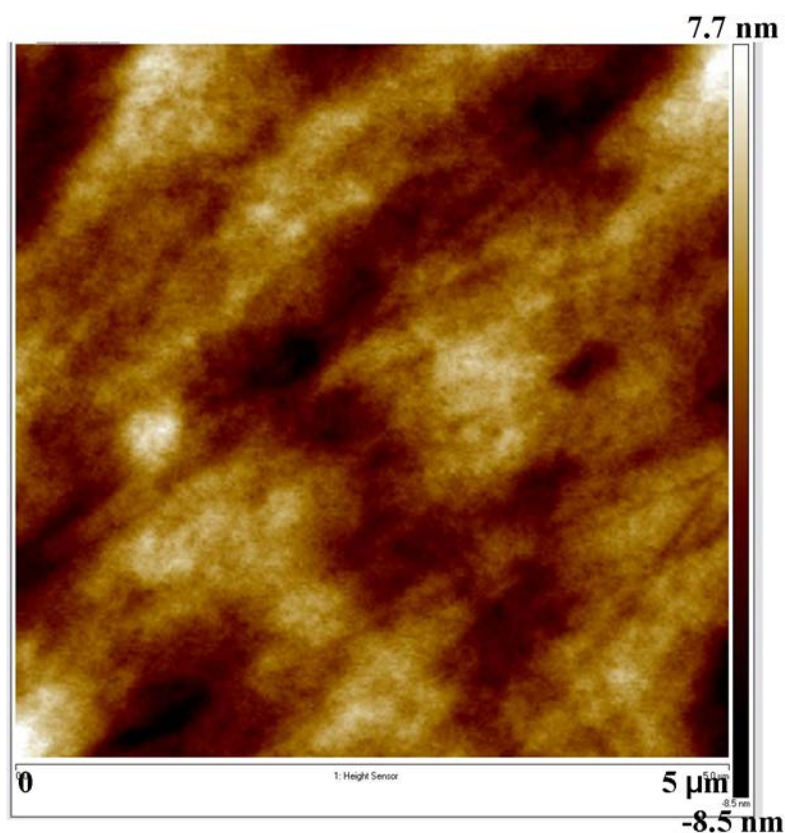


Fig. S6 Probing surface roughness using atomic force microscopy at an area of 25

μm^2 .

5. Low-cost fabrication of hybrid microfluidic device using knives (blades)

To further improve the cost effectively of the developed approach, we fabricated hybrid microfluidic devices manually using two blades. Firstly, we fabricated microchannels of different widths with the aid of a spacer (**Fig. S7**). No spacer (group 1), one spacer (group 2) and two spacers (group 3) were used to incise paper respectively. The spacer used here is a double side adhesive tape with 300 μm thickness (This tape is different from the one used to fabricate microchannel, and can be bought in stationary shops). The channel was imaged using digital microscope (VHX-600, Keyence Corporation, Japan) and analyzed using IPP. All the experiments were repeated 3 times and the result showed that the width were $378 \pm 39 \mu\text{m}$, 696 ± 22 , $1002 \pm 47 \mu\text{m}$ for group 1, 2 and 3, respectively. In group 1 where two blades adhered to each other without a spacer, the channel width was about 378 μm , which results from the distance between the cutting edges. Finally, we fabricated microchannels of different designs, including a straight channel, a trilateral channel and a quadrilateral channel, and we perfused them with red dye. (**Fig. S8**).

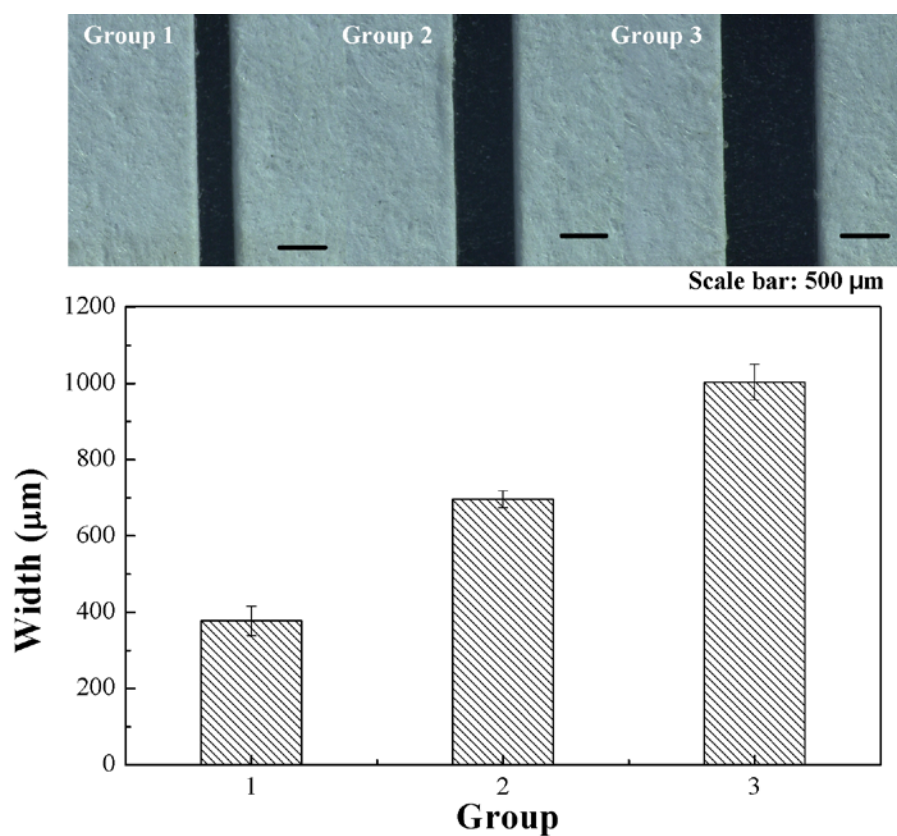


Fig. S7 Characterization of microchannel fabricated manually using two blades with a spacer. Top: Photos of microchannels. No spacer, 1 spacer and 2 spacers were used in group 1, 2 and 3 respectively. Bottom: Quantification of channel widths in three groups.

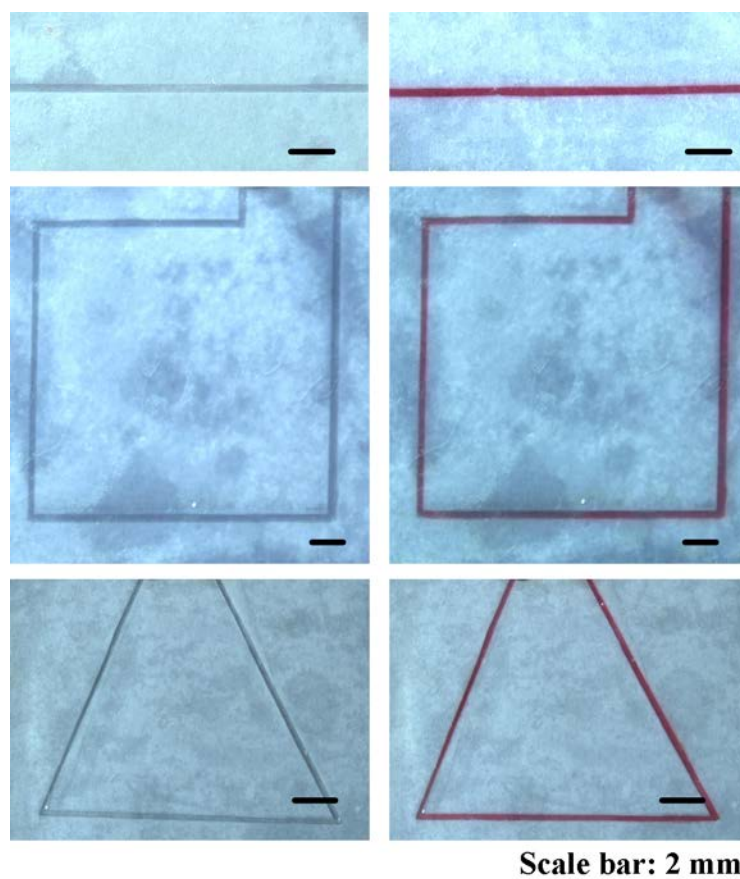


Fig. S8 Photos of microchannels with different patterns fabricated manually and perfused with red dye.